DOI: 10.1002/chem.200903108

Magnetic Coupling in Enantiomerically Pure Trinuclear Helicate-Type Complexes Formed by Hierarchical Self-Assembly

Markus Albrecht,*[a] Marcel Fiege,[a] Paul Kögerler,[b] Manfred Speldrich,[b] Roland Fröhlich,[c] and Marianne Engeser[d]

Abstract: Based on chiral, enantiomerically pure 7-[(*S*)-phenylethylurea]-8-hydroxyquinoline (**1**-H), trinuclear helicate-type complexes **2**–**5** are formed with divalent transition-metal cations. X-ray structural analyses reveal the connection of two monomeric complex units $[M(\mathbf{1})_3]^-$ (M = Zn, Mn, Co, Ni) by a central metal ion to form a "dimer". Due to the enantiopurity of the ligand, the complexes are obtained as pure enantiomers, resulting in pronounced circular dichroism (CD) spectra. Single-ion effects and intra- and intermolecular coupling are observed with dominating ferromagnetic coupling in the case of the cobalt(II) and nickel(II) and dominating antiferromagnetic coupling in the case of the manganese(II) complex.

Keywords: chirality · coordination compounds · helicates · magnetic properties · self-assembly

Introduction

Over the last two decades, the chemistry of helicates has developed into a vivid field of research that addresses the problems of self-assembly processes, supramolecular stereochemistry, and supramolecular functionality.[1] In this context, the study of helicates opens up the opportunity to understand complicated supramolecular phenomena by the investigation of relatively simple chemical systems.[2]

In the first publication on "helicates" by Lehn, this class of complexes was defined as coordination compounds in which two (or three) ligand strands are wrapped around a linear arrangement of two or more metal ions. The oligonuclear coordination compounds are obtained in a "spontaneous" self-assembly processes by simple mixing of the ligands and the metals in solution. Double (or triple) stranded helicates are formed depending on the coordination geometry of the metal ion and on the denticity of the ligand units.[3]

Built on Lehn's first definition, modified systems were developed over the years. Examples are circular helicates,[4] *meso*-helicates[5]/mesocates,[6] cluster helicates,[7] or heteronuclear helicates.[8] Recently, the properties of helicates came into the focus and were specifically tuned to get functional entities. The induced supramolecular function either depends on the special properties of the ligands (e.g. chirality,[9] bioactivity,[10] and *meso*-phase behavior[11]) and/or of the metals (photophysical properties[12] and magnetism[13]).

"Classical" helicates are formed by the self-assembly of oligotopic ligands in the presence of two (or more) metal centers, as is shown in Scheme 1a. As an alternative approach, we recently investigated the hierarchical assembly of triple-stranded helicates.[14] Hereby, three monotopic ligands in an initial step bind to one metal center, forming a classical "Werner-type" coordination compound. If the complex itself possesses additional coordination sites, it can bind to further metal ions, which might act as connectors between two "monomeric" complex moieties (Scheme 1b).

In the literature examples, the connection of the mononuclear units proceeds either by coordination of three metal ions (Scheme 1b1), each bridging to one ligand unit of the respective complex moiety. This is, for example, observed in

[a] Prof. Dr. M. Albrecht, Dr. M. Fiege
Institut für Organische Chemie
RWTH Aachen University, Landoltweg 1
52074 Aachen (Germany)
Fax: (+49) 241-8092385
E-mail: markus.albrecht@oc.rwth-aachen.de

[b] Prof. Dr. P. Kögerler, Dr. M. Speldrich
Institut für Anorganische Chemie
RWTH Aachen University, Landoltweg 1
52074 Aachen (Germany)

[c] Dr. R. Fröhlich
Institut für Organische Chemie
Universität Münster, Corrensstrasse 40
48149 Münster (Germany)

[d] Dr. M. Engeser
Kekule-Institut für Organische Chemie und Biochemie
Universität Bonn, Gerhard-Domagk-Strasse 1
53121 Bonn (Germany)

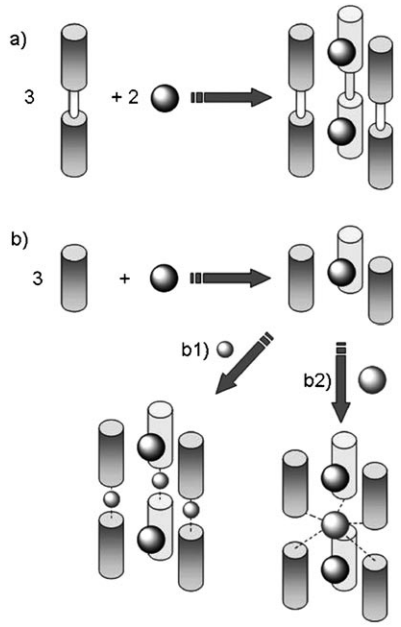

Scheme 1. Schematic representation of the self-assembly of triple-stranded dinuclear helicates (a) and of the hierarchical assembly of helicates (b) (for clarity only the overall connectivity but not the helical arrangement is shown). In the latter case, "dimerization" by the binding of three (b1) or one (b2) metal ion follows the initial formation of a mononuclear complex.

the complexes shown in Scheme 2.[14] As an alternative, only one central metal might act as a template and it connects two mononuclear complex units to obtain helicates (Scheme 1b2).[15] Examples for this motif were frequently observed (for a selection, see Scheme 3).[16]

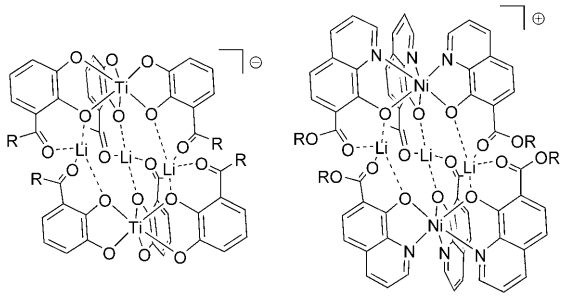

Scheme 2. Two examples of triple-stranded helicates in which three lithium cations are connecting two transition-metal complex units. The lithium ions thus represent the spacer of a linear dicatechol or di-8-quinolinate ligand.

Trinuclear zinc complexes **A** were investigated by our group. In these compounds, two mononuclear tris-8-hydroxyquinolinate zinc complex units (which bear amide or urea moieties at the 7-position of the ligand) adopt a geometry with the three ligands orientated *syn* to each other. This leads to an arrangement of the quinolinate oxygen atoms of

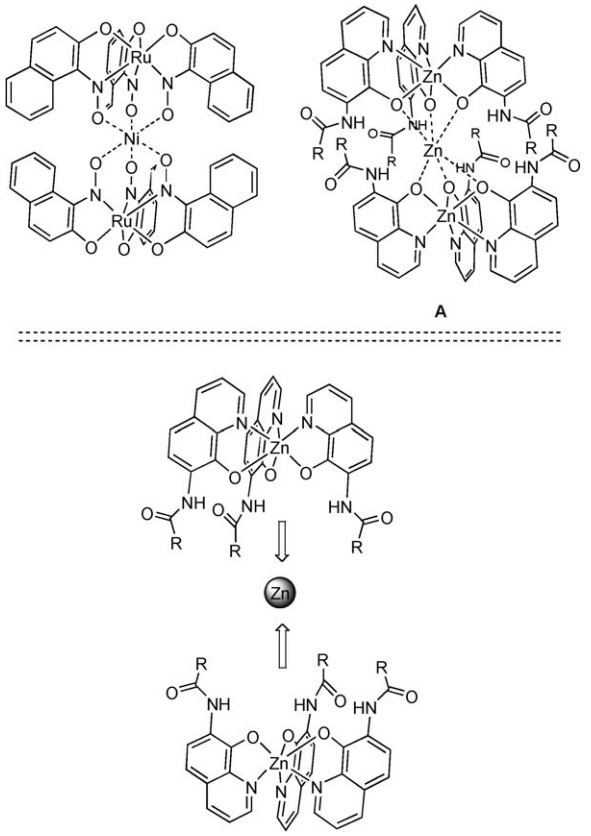

Scheme 3. Examples for hierarchically assembled helicate-type complexes with a central metal ion connecting the two mononuclear complex units. The Aufbau principle is shown on the bottom.

the complex that acts as a tridentate ligand for another metal center. Consequently, coordination of two mononuclear zinc complexes to a central zinc ion forms the trinuclear complex. $[Zn_3(\mathbf{1})_6]$ with an (*S*)-phenylethyl-substituted urea at the 7-position (ligand **1**-H) was structurally characterized. The diffraction study revealed Zn–Zn distances of 2.878 and 2.885 Å and showed intramolecular hydrogen bonds between the urea NH and the quinolinate oxygen atom that probably stabilize the unusual trinuclear structure. Due to the enantiomerically pure ligand, the reported complex is formed as a single enantiomer.[15]

The driving force for the formation of $[Zn_3(\mathbf{1})_6]$ is the electroneutrality of the compound, which makes it soluble in nonpolar solvents, such as chloroform, in which it shows remarkable stability.

The linear arrangement of the three metal ions with metal–metal distances of <3 Å prompted us to examine if we could introduce paramagnetic metal centers. The corresponding studies to form enantiomerically pure trinuclear helicate-type compounds, mass-spectrometric and X-ray crystallographic investigations of obtained compounds, measurements of circular dichroism (CD), and of the magnetic properties are described in this paper.

Results and Discussion

The ligand **1**-H was prepared by the reaction of 7-amino-8-hydroxyquinoline with (*S*)-phenylethylisocyanate. Complex formation proceeded readily by stirring two equivalents of **1**-H with one equivalent of metal(II) acetate in methanol overnight. After removal of the solvent, complexes **2**–**5** were obtained in close to quantitative yield (Scheme 4). The char-

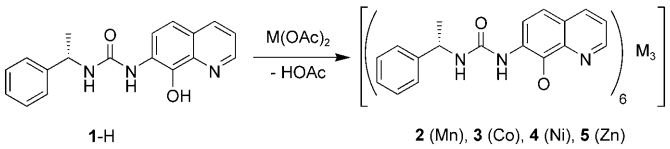

Scheme 4. Preparation of the complexes **2**–**5**.

acterization of the diamagnetic zinc(II) complex **5** in solution and in the solid state was described earlier.[15]

In our hands, NMR spectroscopic investigations of compounds **2**–**4** were not successful, probably due to the paragmagnetism. ESI-MS investigations, on the other hand, revealed the composition of the complexes in solution by detection of their charged adducts with alkali-metal cations. For example, **2** was observed as its doubly sodiated species $[\mathbf{2}][2\,Na]^{2+}$ (m/z: 1023.7692, calcd: 1023.7691) upon electrospray ionization (ESI) in the positive mode. Depending on the choice of solvent and ionization conditions, the singly charged ions $[\mathbf{2}][Na]^+$ and $[\mathbf{2}][H]^+$ are observed as well. In the FTICR spectra, even the complex $\mathbf{2}^{\bullet+}$ appears after longer times of ion accumulation in the hexapole. In addition, species are observed that have lost one or two protonated ligands **1**-H. Collision-induced dissociation (CID) MS/MS experiments with mass-selected $[\mathbf{2}][Na]^+$ confirm the loss of **1**-H as the only primary fragmentation in the gas phase. Subsequently, loss of a second molecule of **1**-H competes with cleavage of the coordinated ligands by consecutive losses of $C_8H_{11}N$ ($\Delta m = 121.09$, phenylethylamine) and of C_9H_9NO ($\Delta m = 147.07$, phenylethylisocyanate). ESI spectra of solutions of **3** in the positive mode are dominated by the sodium adduct of the mononuclear species $[Co(\mathbf{1})_3]$ (m/z: 1000.2974, calcd: 1000.2952). The dinuclear species $[Co_2(\mathbf{1})_6][Na]^+$ is observed in much lower intensities and a signal for a tetranuclear species could not be detected at all.[17] Oxidation to Co^{III} in solution is confirmed by ESI spectra in the negative mode in which a signal for the dinuclear mixed valence species $[Co_2(\mathbf{1})_6]^-$ is visible. Positive-ESI spectra of **4** mainly show characteristic fragments, such as $[Ni(\mathbf{1})_2][Na]^+$, $[Ni_2(\mathbf{1})_3]^+$, $[Ni_2(\mathbf{1})_3][Na]^{2+}$, $[Ni_2(\mathbf{1})_4][Na]^+$, $[Ni_3(\mathbf{1})_4]^{2+}$, $[Ni_3(\mathbf{1})_5]^+$ (m/z: 1704.4331, calcd: 1704.4268), and $[Ni_4(\mathbf{1})_6]^{2+}$. The latter species might be assigned to unfragmented $[\mathbf{4}][Ni]^{2+}$. Further, CID experiments with mass-selected $[Ni_2(\mathbf{1})_4][Na]^+$ confirm the preferred loss of $[Ni(\mathbf{1})_2]$ and of phenylethylamine upon fragmentation in the gas phase; the mass-selected mononuclear product $[Ni_2(\mathbf{1})_3]^+$ finally fragments by three subsequent losses of phenylethylamine cleaving all ligands **1** present in the complex.

We were able to grow X-ray quality crystals of the manganese and cobalt complexes **2** and **3**. The molecular structures in the crystal appear identical on first view, whereas minor differences are only observed upon closer inspection. As a representative example, different views of the manganese(II) complex **2** are shown in Figure 1.

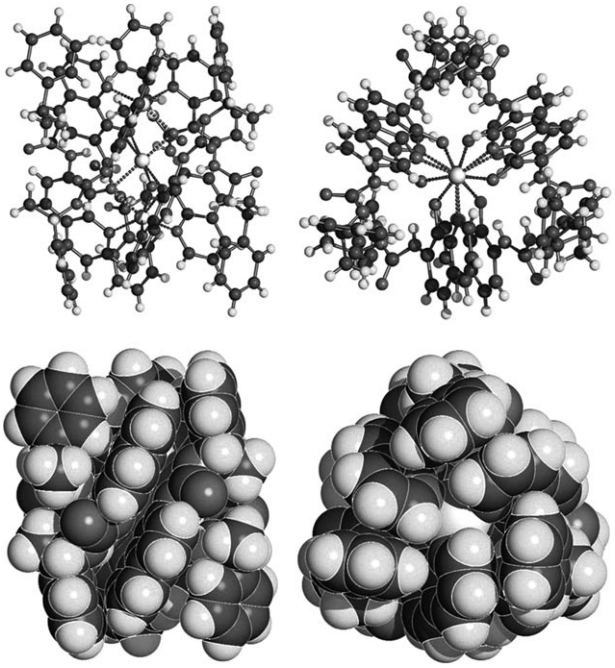

Figure 1. Molecular structure of **2** in the crystal in side (left) and top view (right). Ball and stick (top) and space-filling (bottom) models are shown.

The three metal ions are linearly arranged with M–M distances of less than 3 Å. The six ligands wrap around the metal ions forming a right-handed "hexa-stranded" helix. The orientation of the ligands is alternating (up-down-up-down-up-down). The build-up principle is exemplified for the zinc complex in Scheme 3, bottom. The skeleton of compound **2** revealing only the coordination environment around manganese is depicted in Figure 2 and corresponding selected distances and angles of all compounds are given in Table 1.

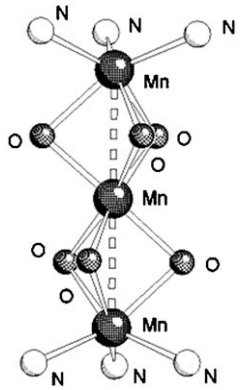

Figure 2. The coordination environment at the metal centers of the trinuclear manganese complex **2**.

All three metal centers possess distorted octahedral coordination geometries. The manganese compound **2** exhibits the longest metal···metal separation, whereas for cobalt complex **3** the shortest is observed

Table 1. Selected distances [Å] and angles [°] around the metal centers of the trinuclear complexes **2**, **3**, and **5**.

	2 (M = Mn)	**3** (M = Co)	**5** (M = Zn)
M···M	2.954(1), 2.952(2)	2.820(2), 2.815(2)	2.885, 2.878
M···M···M	179.90(3)	179.94(9)	179.36
N–M	2.178(4)–2.200(4)	2.059(8)–2.118(8)	2.034–2.096
O–M_{termin}	2.213(3)–2.240(3)	2.076(6)–2.132(7)	2.139–2.180
O–M_{center}	2.161(3)–2.190(3)	2.110(6)–2.132(7)	2.055–2.131
M-O-M	84.1(1)–84.7(1)	82.8(2)–84.0(2)	83.78–86.53

(ca. 0.14 Å shorter). All M···M···M arrangements are linear with angles close to 180°.

The metal–nitrogen bonds decrease in the series **2** > **3** > **5**. In case of oxygen–metal bonds there is a difference in bonding to the terminal or the central metal atoms. Bond lengths to the terminal metal ions decrease in the order **2** > **5** > **3**. Those to the central metal are longer for **2** and shorter, but very similar, for **3** and **5**. Angles at the bridging quinolinate oxygen atoms are in the same range for all three complexes.

The bridging quinolinate oxygen atoms are pyramidalized with a deviation of the oxygen–manganese bond (in **2**) from the plane of the quinoline aromatics by approximately 110°. This pyramidalization allows intramolecular hydrogen bonding to the urea NH, which was earlier attributed to contribute to the stabilization of the trinuclear complex.[15]

Complexes **2**, **3**, and **4** were investigated by CD spectroscopy in dioxane. For solubility reasons, the ligand was measured in methanol. In contrast to the complexes, ligand **1**-H does not show signals with strong intensity ($\Delta\varepsilon > 5/-5$) at a wavelength above 250 nm. The CD spectrum of **2** is shown in Figure 3 and is representative for all complexes. The detected spectra are all very similar, which indicates the same stereochemistry for all of the trinuclear coordination compounds in solution. The spectrum shows a signal with a positive Cotton effect at 270 nm and one with a negative Cotton effect at 285 nm. Those two absorptions are assumed to be ligand-centered. A shoulder at 320 and a signal at 420 nm show weak negative Cotton effects. At least the latter one is tentatively assigned to a charge-transfer transition.

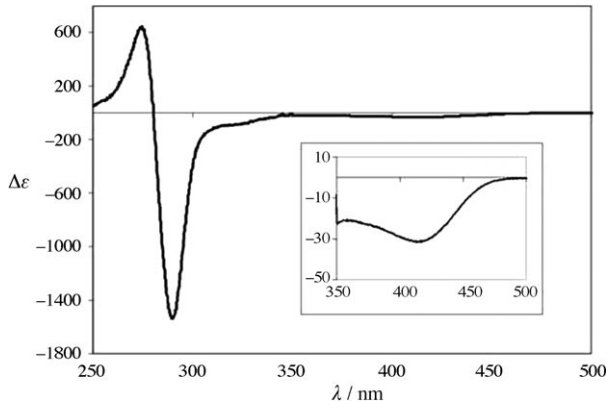

Figure 3. CD spectrum of **2** in dioxane. The inset shows an expansion of the spectrum in the region of charge-transfer transitions.

Based on the X-ray structure analyses of **2**, **3**, and **5**, it is known that the complexes possess a Δ configuration at the metal centers leading to a right-handed "hexa-stranded" helix with alternating orientation of the ligands (see Figure 1).

Earlier NMR spectroscopic investigations with the diamagnetic derivative **5** showed the diastereoselective assembly of only one stereoisomer. Therefore, the complexes with the chiral ligand **1**-H are considered to be enantiomerically pure (within the accuracy of NMR spectroscopy).[15]

Just recently, a trinuclear manganese(IV) complex **B** was reported that possesses a ground spin state of $S = 9/2$ due to ferromagnetic coupling.[18] Therefore, we expected interesting magnetic characteristics for the trinuclear complexes **2**–**5** (Scheme 5).

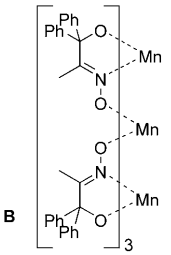

Scheme 5. A trinuclear manganese(IV) complex with the ground spin state $S = 9/2$.

Magnetic properties: The magnetochemical analysis of Co^{II} complexes is frequently complicated by a multitude of factors, notably the fact that the Co^{II} free-ion ^4F ground term is separated by the first excited term ^4P by more than 10^4 cm^{-1}.[19] In a weak ligand field with octahedral symmetry, the ^4F term splits into the $^4T_1(F)$, $^4T_2$, and $^4A_2$ state, whereas the ^4P term transforms into a $^4T_1(P)$ state. The magnetic properties of Co^{II} ($3d^7$) octahedral high-spin complexes are characterized by a significant temperature dependence of μ_{eff} caused by orbital momentum contributions due to the $^4T_1(F)$ ground state. On the other hand, octahedral high-spin complexes of Mn^{II} and Ni^{II} with an orbital singlet ground state (Mn^{II}: $^6A_1(S)$, Ni^{II}: $^3A_2(F)$) represent near-ideal pure spin systems.[20]

For compounds **2**, **3**, and **5** the following single-ion effects were evaluated: interelectronic repulsion (H_{ee}), spin-orbit coupling (H_{so}), ligand-field effects (H_{lf}), and the applied field (H_{mag}) employing the effective Hamiltonian for a $3d^N$ system, see Equation (1):[21,22]

$$\hat{H} = \underbrace{\sum_{i=1}^{N}\left[-\frac{\hbar^2}{2m_e}\nabla_i^2 + V(r_i)\right]}_{\hat{H}^{(0)}} + \underbrace{\sum_{i>j}^{N}\frac{e^2}{r_{ij}}}_{\hat{H}_{ee}} + \underbrace{\sum_{i=1}^{N}\zeta(r_i)\,\kappa\;\hat{\boldsymbol{l}}_i\cdot\;\hat{\boldsymbol{s}}_i}_{\hat{H}_{so}} + \underbrace{\sum_{i=1}^{N}\sum_{k=0}^{\infty}\left\{B_0^k C_0^k(i) + \sum_{q=2}^{k}\left[B_q^k\left(C_{-q}^k(i) + (-1)^q C_q^k(i)\right)\right]\right\}}_{\hat{H}_{LF}} + \underbrace{\sum_{i=1}^{N}\mu_B(\kappa\,\hat{\boldsymbol{l}}_i + 2\,\hat{\boldsymbol{s}}_i)\cdot\;\boldsymbol{B}}_{\hat{H}_{mag}} \quad (1)$$

Whereas $H^{(0)}$ represents the energy in the central-field approximation, H_{ee} and H_{so} account for interelectronic repulsion and spin-orbit coupling (modified by the orbital reduction factor κ to account for covalent M–L contributions), respectively. The former is taken into account by the Racah parameters B and C, the latter by the one-electron spin-orbit coupling parameter ζ. These sets of interelectronic repulsion parameters and ζ are used as constants in the following calculations. H_{lf} accounts for the electrostatic effect of the ligands in the framework of ligand-field theory on the basis of the global parameters B^k_q. The spherical tensors C^k_q are directly related to the spherical harmonics $C^k_q = \sqrt{4\pi/(2k+1)}Y^k_q$ and the real ligand-field parameters B^k_q (Wybourne notation[23,24]) are given by $A^k_q\langle r^k\rangle$ in which A^k_q represents a numerical constant describing the charge distribution in the environment of the metal ion and $\langle r^k\rangle$ is the radial wave function expectation value. For d electrons the terms in the expansion with $k \leq 4$ are nonzero, all odd-k terms vanish since we consider solely configurations containing equivalent electrons. The values of k and q are limited by the point symmetry of the metal-ion site. The spherically symmetric term $B^0_0C^0_0$ that does not cause any splitting is ignored. Note that in cubic or tetragonal systems only spherical tensors with $k \leq 4$ are relevant. The ligand-field operator with reference to the fourfold rotation axis for the angular part of the wave function reads as in Equation (2):

$$H^{cub}_{LF} = B^4_0 \sum_{i=1}^{N} C^4_0(i) + B^4_4 \sum_{i=1}^{N} (C^4_4(i) + C^4_{-4}(i)) \quad (2)$$

Note: $B^4_4 = \sqrt{5/14}B^4_0$ for cubic systems. The matrix elements of $\hat{H}$, omitting $\hat{H}^0$, are evaluated by applying $\hat{H} = H_{ee} + H_{lf} + H_{so} + H_{mag}$ on the full basis of microstates (252, 120, and 45 functions for Mn^{2+}, Co^{2+}, and Ni^{2+}, respectively). Diagonalization leads to the energies E_n and $|n\rangle$, from which the magnetization and the averaged molar susceptibility $\chi_m = (\chi_x + \chi_y + \chi_z)/3$ and the effective Bohr magneton number $\mu_{eff} = 797.74\ (\chi_m T)^{1/2}$ (SI units) are obtained. Intramolecular exchange interactions between the magnetic centers are modeled by using a Heisenberg-type Hamiltonian.

$$\hat{H}_{ex} = -2J_{ex} \sum_{i<j} \hat{S}_i \hat{S}_j \quad (3)$$

Note that we approximate the ligand-field effects for both the central and the two external M^{II} ions by a single uniform environment to confine the number of free-fitting parameters. Distinguishing between the two different $M^{II}O_6$ (O_h) and $M^{II}O_3N_3$ (D_{3d}) environments would require four additional independent ligand-field parameters.

Fitting procedures of the trinuclear Mn^{II} complex: The temperature dependencies of the reciprocal molar susceptibility (χ_m^{-1}) and μ_{eff} of **2** are presented in Figure 4. The effective magnetic moment at room temperature (5.47 per Mn^{II} ion) is smaller than the expected spin-only value of 5.91 for an isolated $S = 5/2$ center ($g_{iso} = 2.0$). Down to approximately 40 K, the susceptibility follows a Curie–Weiss-type term with a Weiss temperature of $\theta = -57$ K, which indicates an antiferromagnetic exchange interaction. A best-fit is obtained for $J_{ex} = -3.5\ cm^{-1}$ ($SQ = 0.8\,\%$, solid lines in Figure 4). The spin-orbit coupling energy (ζ) was chosen as $347\ cm^{-1}$, the Racah parameters as $B = 825$ and $C = 3400\ cm^{-1}$ based on UV/Vis spectra. Note that the obtained J_{ex} value correlates to the Weiss-temperature $\theta = -59$ K ($\theta = (2S(S+1)/3k_B)\sum^{n}_{i} z_i J_{ex,i}$, in which θ is the Weiss-temperature, z_i is the number of i^{th} nearest neighbors of a given magnetic center, $J_{ex,i}$ represents the exchange interaction between the i^{th} neighbors, and n is the number of neighbors for which $J_{ex,i} \neq 0$[25]).

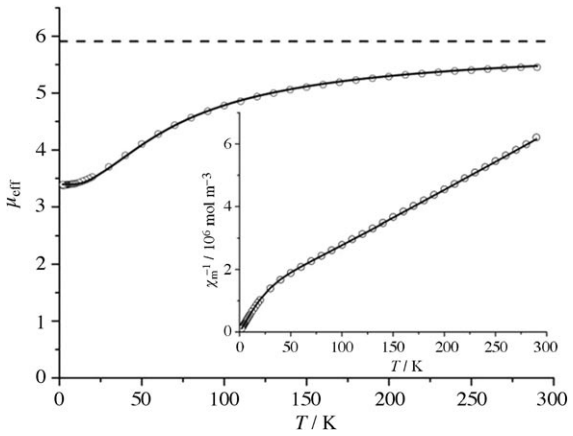

Figure 4. μ_{eff} versus T and χ_m^{-1} versus T plots for **2**, referenced to a single Mn^{II} ion, at an applied field of $B_0 = 0.1$ T. ○: experimental data, ——: best fits for the employed model system. ----- illustrates the pure spin system in the absence of (weak antiferromagnetic) exchange coupling.

Fitting procedures of the trinuclear Co^{II} complex: The effective magnetic moment of the cobalt complex **3** at 290.0 K is 4.72 per Co^{II} ion, slightly smaller than the value resulting for both spin and orbital momentum ($\mu_{LS} = [L(L+1) + 4S(S+1)]^{1/2} = 5.20\ \mu_B$). For octahedral Co^{II} high-spin complexes ($S = 3/2$) in magnetically dilute systems, μ_{eff} values in the range of 4–5 are expected as a result of spin and first-order orbital contributions.[26] Modeling the magnetic behavior, therefore, requires ligand-field effects, spin-orbit coupling, and exchange coupling all be taken into account. To limit the number of free parameters, we restrict the modeling procedure to a uniform ligand-field environment for all three Co sites in **3**. The values for the spin-orbit coupling energy and the Racah parameters were chosen as $\zeta = 426$, $B = 780$, and $C = 3680\ cm^{-1}$ based on UV/Vis spectra.[26]

The parameters J_{ex} and B^4_0 are then fitted to the low-field susceptibility data to yield $J_{ex} = +1.7$ and $B^4_0 = 20\ 000\ cm^{-1}$ ($SQ = 1.3\,\%$ for $T = 14$–290 K). Note that the intramolecular exchange in **3**, mediated by three μ-oxo sites per Co–Co contact ($Co(\mu\text{-}O)_3Co(\mu\text{-}O)_3Co$) is surprisingly similar to the value of $J_{ex} = +1.4\ cm^{-1}$ found for a different Co^{II}_3 molecule with a central $Co(\mu\text{-}O)_2(\mu\text{-}COO)Co(\mu\text{-}O)_2(\mu\text{-}COO)Co$ motif despite significantly larger Co···Co distances of 3.27 Å.[27]

Note that weak additional antiferromagnetic coupling (possibly between the outer Co centers) causes a gradual decrease of μ_{eff} below approximately 15 K (Figure 5).

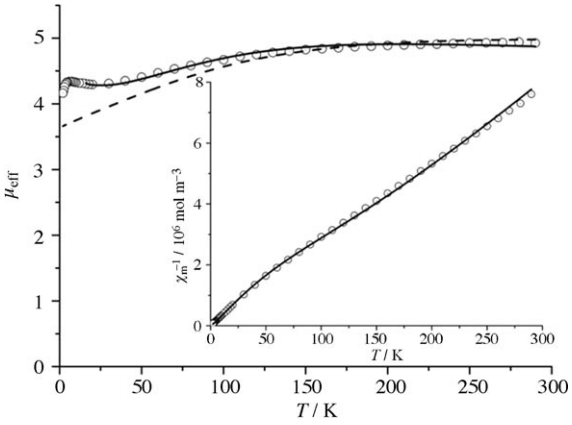

Figure 5. μ_{eff} versus T and $\chi_m{}^{-1}$ versus T plots for **3**, referenced to a single Co^{II} ion, at an applied field of $B_0 = 0.1$ T. ○: experimental data, ——: best fits for the employed model system. ----- illustrates the single-ion contributions of uncoupled Co^{II}-centers in the absence of (weak ferromagnetic) exchange coupling.

Fitting procedures of the trinuclear Ni^{II} complex: The effective magnetic moment of the nickel complex **4** at room temperature is 3.4 per Ni^{II} ion, significantly larger than the expected spin-only value for an isolated nickel center ($S=1$) of 2.83 μ_B for $g=2.0$. The susceptibility data display Curie Weiss-type behavior in the temperature range of 50 to 300 K with a Curie constant $C = 1.829 \times 10^{-5}$ m^3 K mol^{-1} ($\mu = 3.41$ μ_B) in good agreement with the expected value for an isolated paramagnetic Ni^{2+} ion in an octahedral coordination environment.[28] The observed increase of μ_{eff} with decreasing temperatures up to a maximum of around 3.98 at 7 K suggests ferromagnetic intramolecular coupling (Figure 6). At lower temperatures, antiferromagnetic interactions (likely caused by through-space intermolecular coupling) become more dominant.

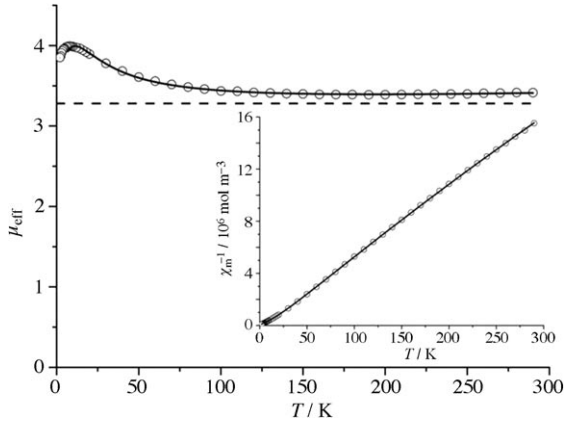

Figure 6. μ_{eff} versus T and $\chi_m{}^{-1}$ versus T plots for **4**, referenced to a single Ni^{II} ion ($B_0 = 0.1$ T). ○: experimental data, ——: best fits for the employed model system. ----- illustrates the uncoupled Ni^{II} centers.

The multidimensional intermolecular exchange interactions between the trinuclear units are modeled by using a phenomenological approach, the molecular-field approximation:

$$\chi_m^{-1}\chi'^{-1}_m(B,C,\zeta,B_q^k J_{ex}) - \lambda_{mf} \quad (4)$$

in which χ'_m denotes the susceptibility per Ni^{II} ion and λ_{mf} the molecular-field parameter. Positive and negative values for λ_{mf} correlate with dominant ferromagnetic and antiferromagnetic interactions, respectively, between the trinuclear units. With set values for the spin-orbit coupling energy ($\zeta = 649$ cm^{-1}) and the Racah parameters ($B = 1048$ cm^{-1}, $C = 4183$ cm^{-1}) the parameters J_{ex}, B_0^4, and λ_{mf} are determined by least-squares fitting.[19c] The best fit to the susceptibility values was found for $J_{ex} = +6.1$ cm^{-1}, $B_0^4 = 21\,000$ cm^{-1}, and $\lambda_{mf} = -6.061 \times 10^4$ mol m^{-3} ($SQ = 0.4\,\%$ for $T = 10$–290 K).

Conclusion

In this paper we presented the formation and structures of trinuclear helicate-type complexes. They are built up from metal(II) trisquinolinate units that are connected by a central metal(II) ion. Thus the compounds are neutral and are well soluble in organic solvents. Due to the enantiopurity of the ligand **1**-H, the coordination compounds are obtained in an enantiomerically pure form (S-ligand→right-handed helix). Due to the proximity of the three metal centers, dominating intramolecular magnetic coupling is observed in the case of the nickel(II) (ferromagnetic), cobalt(II) (weak ferromagnetic), and manganese(II) (antiferromagnetic) complexes. However, single-ion effects and intermolecular coupling additionally influence the magnetic behavior. In this paper we have presented a supramolecular system in which hierarchical self-assembly affords enantiomerically pure trinuclear coordination compounds possessing interesting magnetic properties. Although the three major aspects of this study (chirality, magnetism, hierarchical assembly) are not directly connected, they are all worth discussing. At the moment we are trying to modify the properties of the compounds by modification of the organic ligand part.

Experimental Section

General: NMR spectra were recorded on a Varian Mercury 300 or Inova 400 spectrometer. FTIR spectra were recorded by using a Bruker IFS spectrometer. Elemental analyses were obtained on a Heraeus CHN-O-Rapid analyzer. UV measurements were performed on a Varian Cary 3E spectrometer. CD spectra were detected by using a Lakewood 62DS spectrometer. ESI mass spectra were recorded with a Bruker micrOTOF-Q and a Bruker Apex IV FTICR mass spectrometer equipped with Apollo ESI sources by using 10^{-4} M acetonitrile or methanol solutions. Argon was used as a collision gas for CID measurements.

X-ray crystallography: Data sets were collected with a Nonius KappaCCD diffractometer, equipped with a rotating anode generator. Programs used: data collection COLLECT (Nonius B.V., 1998), data reduction Denzo-SMN,[29] absorption correction SORTAV[30] and Denzo,[31] structure solution SHELXS-97,[32] structure refinement SHELXL-97,[33] and graphics SCHAKAL (E. Keller, 1997). CCDC-752273 and 752274 contain the supplementary crystallographic data for this paper. These data can be obtained free of charge from The Cambridge Crystallographic Data Centre via www.ccdc.cam.ac.uk/data_request/cif.

Magnetic measurements: Magnetic susceptibility data were determined by SQUID magnetometry (Quantum Design MPMS-5XL) in the temperature range $T=2.0$ to 290 K and at an applied field of $B_0=0.1$ T. The data were corrected for the sample holder (Teflon capsules) and calculated diamagnetic contributions amount to $\chi_{dia}=-12.5\times10^{-9}\ m^3mol^{-1}$ for all three compounds.[34,35]

General procedure for the preparation of metal(II) complexes of the 8-hydroxyquinoline ligand 1-H: 1-(8-Hydroxyquinolin-7-yl)-3-[(*S*)-1-phenylethyl]urea (**1**-H) was prepared in a four-step procedure by starting from 8-hydroxyquinoline-5-sulfuric acid as described in the literature. Ligand **1**-H (2 equiv) and zinc(II) acetate, nickel(II) acetate, cobalt(II) acetate, or manganese (II)acetate (1 equiv) were dissolved in methanol and stirred overnight under reflux. The solvent was removed under reduced pressure to give the solid complexes in close to quantitative yields.

*[Mn$_3$(**1**)$_6$] (**2**)*: Light-green solid; yield: 52 mg (96%); m.p. >250°C (decomp.); IR (KBr): $\tilde{\nu}=3402$, 3309, 2968, 1696, 1602, 1527, 1498, 1445, 1365, 1320, 1294, 1252, 1193, 1100, 1075, 824, 749, 701, 674, 583 cm^{-1}; UV (dioxane): $\lambda=212$, 280, 413 nm; positive HR-ESI MS: *m*/*z*: calcd: 1023.7691; found: 1023.7692, correct isotope pattern for $[Mn_3(\mathbf{1})_6][Na_2]^{2+}$; elemental analysis calcd (%) for $C_{108}H_{96}N_{18}O_{12}Mn_3{\cdot}5H_2O$: C 60.93, H 5.21, N 11.84; found: C 61.03, H 4.93, N 11.30.

*X-ray crystal structure analysis of [Mn$_3$(**1**)$_6$]*: Formula = $C_{108}H_{96}Mn_3N_{18}O_{12}$; $M=2002.85$; orange/red crystal; $0.35\times0.30\times0.20$ mm; $a=14.7405(2)$, $b=18.1550(3)$, $c=21.8433(4)$ Å; $\beta=108.341(1)°$; $V=5548.62(16)$ Å^3; $\rho_{calcd}=1.199$ g cm^{-3}; $\mu=0.400$ mm^{-1}; empirical absorption correction ($0.873\le T\le0.924$); $Z=2$; monoclinic; space group = $P2_1$ (No. 4); $\lambda=0.71073$ Å; $T=223(2)$ K; ω and ϕ scans; 29513 reflections collected ($\pm h$, $\pm k$, $\pm l$), $[(\sin\theta)/\lambda]=0.60$ Å^{-1}, 17294 independent ($R_{int}=0.040$) and 12080 observed reflections [$I\ge2\sigma(I)$], 1294 refined parameters, $R=0.056$, $wR^2=0.140$; Flack parameter = 0.009(14); max. (min.) residual electron density = 0.35 (−0.26) e Å^{-3}; hydrogen atoms at N from difference fourier maps, others calculated and refined as riding atoms, all N–H distances refined with geometrical (SADI), groups C27–C33 and C87–C93 with geometrical (AFIX 66) and thermal (ISOR) restraints, solvents in voids couldn′t be assigned; therefore, the SQUEEZE routine was applied.

*[Co$_3$(**1**)$_6$] (**3**)*: Light-brown solid; yield: 54 mg (99%); m.p. >250°C (decomp.); IR (KBr): $\tilde{\nu}=3550$, 3377, 3059, 3028, 2971, 1673, 1600, 1536, 1501, 1455, 1422, 1369, 1320, 1262, 1198, 1137, 1109, 1072, 825, 757, 701, 669, 564 cm^{-1}; UV (dioxane): $\lambda=212$, 276, 413 nm; positive HR-ESI MS: *m*/*z*: calcd: 1977.6011; found: 1977.5915, correct isotope pattern for $[Co^{III}_2(\mathbf{1})_6][Na]^{+}$; elemental analysis calcd (%) for $C_{108}H_{96}N_{18}O_{12}Co_3{\cdot}4H_2O$: C 62.16, H 5.02, N 12.08; found: C 61.90, H 5.10, N 11.74.

*X-ray crystal structure analysis of [Co$_3$(**1**)$_6$]*: Formula = $C_{108}H_{96}Mn_3N_{18}O_{12}$; $M=2014.82$; red crystal $0.40\times0.20\times0.10$ mm; $a=14.7592(4)$, $b=18.0766(5)$, $c=21.6902(6)$ Å; $\beta=108.607(2)°$; $V=5484.4(3)$ Å^3; $\rho_{calcd}=1.220$ g cm^{-3}; $\mu=0.513$ mm^{-1}; empirical absorption correction ($0.821\le T\le0.951$); $Z=2$; monoclinic; space group = $P2_1$ (No. 4); $\lambda=0.71073$ Å; $T=223(2)$ K; ω and ϕ scans; 26324 reflections collected ($\pm h,\pm k,\pm l$); $[(\sin\theta)/\lambda]=0.54$ Å^{-1}; 13268 independent ($R_{int}=0.084$) and 9524 observed reflections [$I\ge2\sigma(I)$], 1198 refined parameters, $R=0.081$, $wR^2=0.225$; Flack parameter 0.08 (2), max. (min.) residual electron density = 0.59 (−0.43) e Å^{-3}; hydrogen atoms calculated and refined as riding atoms, groups C18–C23 of molecules C, D, and E refined with geometrical (AFIX 66) and thermal (ISOR) restraints, solvents in voids couldn′t be assigned; therefore, the SQUEEZE routine was applied.

*[Ni$_3$(**1**)$_6$] (**4**)*: Light-green solid; yield: 53 mg (98%); m.p. >250°C (decomp.); IR (KBr): $\tilde{\nu}=3961$, 3914, 3871, 3854, 3652, 3630, 3344, 3053, 3029, 2969, 2930, 1691, 1605, 1534, 1502, 1448, 1426, 1368, 1319, 1258, 1218, 1192, 1136, 1101, 909, 826, 787, 750, 700, 676, 587, 543 cm^{-1}; UV (dioxane): $\lambda=212$, 277, 413 nm; positive HR-ESI MS: *m*/*z*: calcd: 1704.4268; found: 1704.4331, correct isotope pattern for $[Ni_3(\mathbf{1})_5]^{+}$; elemental analysis calcd (%) for $C_{108}H_{96}N_{18}O_{12}Ni_3{\cdot}7H_2O$: C 60.61, H 5.18, N 11.78; found: C 60.35, H 4.89, N 11.42.

*[Zn$_3$(**1**)$_6$] (**5**)*: Prepared as described in the literature.[15]

Acknowledgements

Financial support by the Deutsche Forschungsgemeinschaft and the Fonds der Chemischen Industrie is gratefully acknowledged. We thank Prof. Dr. G. Raabe for measurement of the CD spectra.

[1] Reviews: a) C. Piguet, G. Bernardinelli, G. Hopfgartner, *Chem. Rev.* **1997**, *97*, 2005; b) M. Albrecht, *Chem. Rev.* **2001**, *101*, 3457; c) M. J. Hannon, L. J. Childs, *Supramol. Chem.* **2003**, *16*, 7; d) M. Albrecht, *Angew. Chem.* **2005**, *117*, 6606–6609; *Angew. Chem. Int. Ed.* **2005**, *44*, 6448–6451.

[2] a) J.-M. Lehn, *Supramolecular Chemistry—Concepts and Perspectives*, Wiley-VCH, Weinheim **1995**; b) G. M. Whitesides, J. P. Mathias, C. T. Seto, *Science* **1991**, *254*, 1312; c) D. Philp, J. F. Stoddart, *Angew. Chem.* **1996**, *108*, 1242; *Angew. Chem. Int. Ed. Engl.* **1996**, *35*, 1154; d) J. S. Lindsey, *New J. Chem.* **1991**, *15*, 153; M. Albrecht, *Naturwissenschaften* **2007**, *94*, 951–966; e) R. W. Saalfrank, H. Maid, A. Scheurer, *Angew. Chem.* **2008**, *120*, 8924–8956; *Angew. Chem. Int. Ed.* **2008**, *47*, 8794–8824.

[3] J.-M. Lehn, A. Rigault, J. Siegel, J. Harrowfield, B. Chevrier, D. Moras, *Proc. Natl. Acad. Sci. USA* **1987**, *84*, 2565.

[4] B. Hasenknopf, J.-M. Lehn, B. O. Kneisel, G. Baum, D. Fenske, *Angew. Chem.* **1996**, *108*, 1987–1990; *Angew. Chem. Int. Ed. Engl.* **1996**, *35*, 1838–1840.

[5] a) M. Albrecht, *Chem. Eur. J.* **2000**, *6*, 3485; b) M. Albrecht, S. Kotila, *Angew. Chem.* **1995**, *107*, 2285; *Angew. Chem. Int. Ed. Engl.* **1995**, *34*, 2134.

[6] J. Xu, T. N. Parac, K. N. Raymond, *Angew. Chem.* **1999**, *111*, 3055; *Angew. Chem. Int. Ed.* **1999**, *38*, 2878.

[7] J. Sanmartín, M. R. Bermejo, A. M. Garcia-Deibe, O. Piro, E. E. Castellano, *Chem. Commun.* **1999**, 1953–1954.

[8] a) C. Piguet, G. Hopfgartner, A. F. Williams, J.-C. G. Bünzli, *J. Chem. Soc. Chem. Commun.* **1995**, 491–492; b) M. Albrecht, R. Fröhlich, *J. Am. Chem. Soc.* **1997**, *119*, 1656–1661.

[9] a) W. Zarges, J. Hall, J.-M. Lehn, C. Bolm, *Helv. Chim. Acta* **1991**, *74*, 1843; b) A. Lützen, M. Hapke, J. Griep-Raming, D. Haase, W. Saak, *Angew. Chem.* **2002**, *114*, 2190; *Angew. Chem. Int. Ed.* **2002**, *41*, 2086; c) M. Albrecht, S. Schmid, M. deGroot, P. Weis, R. Fröhlich, *Chem. Commun.* **2003**, 2526; d) M. Albrecht, I. Janser, J. Fleischhauer, Y. Wang, G. Raabe, R. Fröhlich, *Mendeleev Commun.* **2004**, 14, 250.

[10] I. Meistermann, V. Moreno, M. J. ;Prieto, E. Moldrheim, E. Sletten, S. Khalid, P. M. Rodger, J. C. Peberdy, C. J. Isaac, A. Rodger, M. J. Hannon, *Proc. Natl. Acad. Sci. USA* **2002**, *99*, 5069–5074.

[11] a) R. Ziessel, *Coord. Chem. Rev.* **2001**, *216/217*, 195–223; b) A. El-Ghayouy, L. Douce, A. Skoulios, R. Ziessel, *Angew. Chem.* **1998**, *110*, 2327–2331; *Angew. Chem. Int. Ed.* **1998**, *37*, 2205–2208.

[12] a) C. Piguet, J.-C. G. Bünzli, *Chem. Soc. Rev.* **1999**, *28*, 347; b) J.-C. G. Bünzli, C. Piguet, *Chem. Soc. Rev.* **2005**, *34*, 1048; c) M. Albrecht, O. Osetska, R. Fröhlich, J.-C. G. Bünzli, A. Aebischer, F. Gumy, J. Hamacek, *J. Am. Chem. Soc.* **2007**, *129*, 14178–14179.

[13] C. Piguet, E. Rivara-Minten, G. Hopfgartner, J.-C. G. Bünzli, *Helv. Chim. Acta* **1995**, *78*, 1651–1672.

[14] a) M. Albrecht, S. Mirtschin, M. de Groot, I. Janser, J. Runsink, G. Raabe, M. Kogej, C. A. Schalley, R. Fröhlich, *J. Am. Chem. Soc.* **2005**, *127*, 10371; b) M. Albrecht, M. Baumert, J. Klankermayer, M. Kogej, C. A. Schalley, R. Fröhlich, *Dalton Trans.* **2006**, 4395; c) M.

Albrecht, M. Fiege, M. Baumert, M. de Groot, R. Fröhlich, L. Russo, K. Rissanen, *Eur. J. Inorg. Chem.* **2007**, 609–616.
[15] a) M. Albrecht, K. Witt, H. Röttele, R. Fröhlich, *Chem. Commun.* **2001**, 1330; b) M. Albrecht, K. Witt, P. Weis, E. Wegelius, R. Fröhlich, *Inorg. Chim. Acta* **2002**, *341*, 25; c) M. Albrecht, M. Fiege, O. Osetska, *Coord. Chem. Rev.* **2008**, *252*, 812–824.
[16] a) A. K. Das, A. Rueda, L. R. Falvello, S.-M. Peng, S. Batthacharya, *Inorg. Chem.* **1999**, *38*, 4365; b) J. Heinicke, N. Peulecke, K. Karaghiosoff, P. Mayer, *Inorg. Chem.* **2005**, *44*, 2137; c) T. Konno, K. Tokuda, T. Suzuki, K. I. Okamoto, *Bull. Chem. Soc. Jpn.* **1998**, *71*, 1049; d) T. Konno, K. Tokuda, K. Okamoto, *Chem. Commun.* **1998**, 1697; e) M. H. W. Lam, S. T. C. Cheung, K.-M. Fung, W.-T. Wong, *Inorg. Chem.* **1997**, *36*, 4618.
[17] Several additional series of signals with $\Delta m = 117.100$ are observed due to the presence of trace amounts of a nitro derivative ($C_9H_6N_2O_3$) that stems from the synthesis of the ligand.
[18] a) T. Pathmalingam, S. I. Gorelsky, T. J. Burchell, A.-C. Bedard, A. M. Beauchemin, R. Clerac, M. Murugesu, *Chem. Commun.* **2008**, 2782–2784; b) for another example of paramagnetic helicates, see: R. W. Saalfrank, A. Dresel, V. Seitz, S. Trummer, F. Hampel, M. Teichert, D. Stalke, C. Stadler, J. Daub, V Schunemann, A. F. Trautwein, *Chem. Eur. J.* **1997**, *3*, 2058–2062.
[19] a) B. N. Figgs and M. A. Hitchman, *Ligand-Field Theory and its Applications*, Wiley-VCH, New York, **2000**; b) C. J. Ballhausen, *Introduction to Ligand-Field Theory*, McGraw-Hill, New York, **1962**; c) J. S. Griffith. *The Theory of Transition-Metal Ions*, Cambridge University Press, Cambridge,.
[20] O. Kahn, *Molecular Magnetism*, VCH, Weinheim, **1993**.
[21] S. Hatscher, H. Schilder, H. Lueken, W. Urland, *Pure Appl. Chem.* **2005**, *77*, 497–511.
[22] H. Schilder, H. Lueken, *J. Magn. Magn. Mater.* **2004**, *281*, 17–26.
[23] B. G. Wybourne, *Spectroscopic Properties of Rare Earths*, Wiley, New York, **1965**.
[24] C. Gorller-Walrand, K. Binnemans, *Rationalization of crystal-field parametrization in Handbook on the Physics and Chemistry of Rare Earths, Vol. 23* (Eds.: K. A. Gschneidner, Jr., L. Eyring), Elsevier, Amsterdam, **1996**, Chapter 155, p. 121.
[25] J. S. Smart . *Effective Field Theories of Magnetism*, Saunders, Philadelphia, **1966**.
[26] a) E. König, S. Kremer, *Magnetism Diagrams for Transition Metal Ions*; Plenum Press, New York, **1979**; b) A. B. P. Lever, *Inorganic Electronic Spectroscopy*, Elsevier, Amsterdam, **1984**.
[27] I. L. Malaestean, M. Speldrich, S. G. Baca, A. Ellern, H. Schilder, P. Kögerler, *Eur. J. Inorg. Chem.* **2009**, 1011.
[28] F. E. Mabbs, D. J. Machin, *Magnetism and Transition Metal Complexes*, Chapman and Hall, London, **1973**.
[29] Z. Otwinowski, W. Minor, *Methods in Enzymology*, **1997**, *276*, 307–326.
[30] a) R. H. Blessing, *Acta Cryst.* **1995**, *A51*, 33–37; b) R. H. Blessing, *J. Appl. Cryst.* **1997**, *30*, 421–426.
[31] Z. Otwinowski, D. Borek, W. Majewski, W. Minor, *Acta Cryst.* **2003**, *A59*, 228–234.
[32] G. M. Sheldrick, *Acta Cryst.* **1990**, *A46*, 467–473.
[33] G. M. Sheldrick, *Acta Cryst.* **2008**, *A64*, 112–122.
[34] W. Haberditzl, *Angew. Chem.* **1966**, *78*, 277; *Angew. Chem. Int. Ed. Engl.* **1966**, *5*, 288.
[35] H. Lueken, *Magnetochemie*, Teubner, Stuttgart **1999**.

Received: November 12, 2009
Revised: May 19, 2010
Published online: June 25, 2010

